

Regional Hydrology of the Dixie Valley Geothermal Field, Nevada: Preliminary Interpretations of Chemical and Isotopic Data

*G. Nimz, C. Janik, F. Goff, C. Dunlap, M. Huebner,
D. Counce, S. Johnson*

This was prepared for submittal to the
8th International Conference on Accelerator Mass Spectrometry,
Vienna, Austria, September 6-10, 1999

U.S. Department of Energy

Lawrence
Livermore
National
Laboratory

August 16, 1999

DISCLAIMER

This document was prepared as an account of work sponsored by an agency of the United States Government. Neither the United States Government nor the University of California nor any of their employees, makes any warranty, express or implied, or assumes any legal liability or responsibility for the accuracy, completeness, or usefulness of any information, apparatus, product, or process disclosed, or represents that its use would not infringe privately owned rights. Reference herein to any specific commercial product, process, or service by trade name, trademark, manufacturer, or otherwise, does not necessarily constitute or imply its endorsement, recommendation, or favoring by the United States Government or the University of California. The views and opinions of authors expressed herein do not necessarily state or reflect those of the United States Government or the University of California, and shall not be used for advertising or product endorsement purposes.

This is a preprint of a paper intended for publication in a journal or proceedings. Since changes may be made before publication, this preprint is made available with the understanding that it will not be cited or reproduced without the permission of the author.

This report has been reproduced
directly from the best available copy.

Available to DOE and DOE contractors from the
Office of Scientific and Technical Information
P.O. Box 62, Oak Ridge, TN 37831
Prices available from (423) 576-8401
<http://apollo.osti.gov/bridge/>

Available to the public from the
National Technical Information Service
U.S. Department of Commerce
5285 Port Royal Rd.,
Springfield, VA 22161
<http://www.ntis.gov/>

OR

Lawrence Livermore National Laboratory
Technical Information Department's Digital Library
<http://www.llnl.gov/tid/Library.html>

Regional Hydrology of the Dixie Valley Geothermal Field, Nevada: Preliminary Interpretations of Chemical and Isotopic Data

Gregory Nimz¹, Cathy Janik², Fraser Goff³, Charles Dunlap⁴,
Mark Huebner², Dale Counce³, and Stuart Johnson⁵

1 – Lawrence Livermore National Laboratory, Livermore CA 94550

2 – U.S. Geological Survey, Menlo Park CA 94025

3 – Los Alamos National Laboratory, Los Alamos NM 87545

4 – University of California, Santa Cruz CA 95064

5 – Oxbow Power Services Incorporation, Reno NV 89511

Keywords: hydrology, hydrochemistry, isotopes, chlorine, recharge, Dixie Valley

Abstract

Chemical and isotopic analyses of Dixie Valley regional waters indicate several distinct groups ranging in recharge age from Pleistocene (<20 ka) to recent (<50a). Valley groundwater is older than water from perennial springs and artesian wells in adjacent ranges, with Clan Alpine range (east) much younger (most <50a) than Stillwater range (west; most >1000a). Geothermal field fluids (~12-14 ka) appear derived from water similar in composition to non-thermal groundwater observed today in valley artesian wells (also ~14 ka). Geothermal fluid interaction with mafic rocks (Humboldt Lopolith) appears to be common, and significant reaction with granodiorite may also occur. Despite widespread occurrence of carbonate rocks, largescale chemical interaction appears minor. Age asymmetry of the ranges, more extensive interaction with deep-seated waters in the west, and distribution of springs and artesian wells suggest the existence of a regional upward hydrologic gradient with an axis in proximity to the Stillwater range.

Introduction

Dixie Valley is located in the western Basin and Range Province in west-central Nevada between the Stillwater (SW) and Clan Alpine-Augusta (CAA) mountain ranges (Fig. 1). Both the valley and ranges are characterized by artesian wells and abundant perennial springs. The Humboldt Salt Marsh covers a wide area in the center of the valley. The Dixie Valley geothermal field (DVGF) is located in the northwest part of the valley, along the SW range front. Operation of the power plant began in 1988 and has a production of 62 MWe. Fluids are produced from ~2500-3000m depth at a temperature of ~250°C. The present production field covers ~20 km². The Oxbow Geothermal Corporation owns and operates the plant and its geothermal wells.

The purpose of this paper is to discuss chemical and isotopic data obtained from waters in the Dixie Valley and surrounding areas that pertain to the regional hydrologic system, including the geothermal field. Samples were collected from both cold and thermal wells and springs in Dixie Valley and the SW-CAA ranges. Samples were analyzed for elemental compositions, $\delta^{13}\text{C}$, δD , $\delta^{18}\text{O}$, ^{14}C , $^{36}\text{Cl}/\text{Cl}$, and $^{87}\text{Sr}/^{86}\text{Sr}$. The objective is to characterize the hydrologic relations between the regional groundwaters, valley hot springs, and the geothermal production fluids.

Geologic Setting

Dixie Valley basin is bounded on the west by the tectonically active Stillwater Fault (earthquakes in 1915 and 1954, $M \approx 7$; Okaya and Thompson, 1985). The basin is bounded on the east by step

faults, some of which are observed in the valley by linear N-NE trending arrays of springs. Valley sedimentary fill exceeds 2000m in the west and thins towards the CAA range to the east.

The oldest common rocks in the hydrologic basin are Mesozoic marine sequences. In the CAA range, upper Triassic sections occur as thick units of pelites, quartz arenites, clastic and micritic limestones, and dolomites. Lithologically similar sequences of slightly older age (early Triassic) are the oldest rocks in the SW range. The SW upper Triassic section is a thick sequence of pelitic rocks overlain by late Triassic-Jurassic calcareous pelites. Thin units of lower Jurassic, heavily deformed carbonates, calcarenites, and pelitic rocks overlie these or are in thrust fault contact. The Jurassic Humboldt Lopolith overlies the SW-range Triassic section in thrust-fault contact (Speed, 1976). It is of mafic composition (coarse-grained gabbros, picrites, anorthosites), and locally reaches thicknesses in excess of 1200m (Speed, 1976). The entire Mesozoic sequence was intruded by several Cretaceous (69-104 Ma) granodioritic bodies of unknown subsurface extent. They crop out on the lower slopes of the western SW range and are encountered in the footwall of the Stillwater fault by DVGF boreholes (~3300m depth). Moderately thick mid-Cenozoic silicic tuffs occur in both ranges. They are found above the lopolith section in DVGF boreholes. Seismic data indicate depth to pre-Tertiary basement in the valley exceeds ~2500m near the DVGF. Late-Cenozoic basalts cap both ranges, and form areally extensive units. In DVGF boreholes they occur just beneath the valley fill units at ~2100-2400m.

Hydrologic Setting

Dixie Valley is an enclosed basin with a surface drainage of ~5200km² (Parchman and Knox, 1981). Pleistocene-age shorelines and lake deposits exist ("Lake Dixie"), and vertical recharge probably occurred at that time. (Thompson and Burke, 1973; Bell and Katzer, 1990). Today, water enters the basin during winter and spring from streams draining the SW and CAA ranges. Subsurface water movement within the ranges is probably controlled by fracture flow and geologic structure. However, very little is actually known about the hydrology of these ranges.

The valley fill holds an unknown number of aquifers. A shallow unconfined aquifer certainly occurs near the Humboldt Salt Marsh. Irrigation wells in the north valley draw water from deeper basin fill, but the thickness or confinement state of these aquifers is unknown. Dixie settlement domestic wells are under artesian head, implying confinement. Basalts underlying the basin fill host an aquifer that is a secondary DVGF production zone; seismic data indicate they are continuous throughout the valley and dip slightly westward. Tertiary ash-flows underlying the basalts are encountered in DVGF boreholes where they occur as thin units (<200m) with poor aquifer characteristics. They are probably not significant valley aquifers. The intersection of the SW fault zone with the lopolith creates the largest DVGF producing zone. However, boreholes away from the fault zone indicate low permeability in the lopolith, with lower temperature gradients than the overlying volcanic units (Williams et al., 1997). Lopolith lithologies are not naturally porous, and flow must be fracture dominated. Spatially variable hydrologic properties are to be expected. Subsurface aquifer characteristics of the Triassic units are unknown. Cementation often substantially reduces porosity in such lithologies. A borehole penetrating these units north of the DVGF shows low hydraulic pressure and low temperature gradients indicative of low porosity (Williams et al., 1997). Triassic units in the SW and CAA ranges are substantially fractured only where adjacent to major fault zones (Speed, 1976). The Cretaceous granodiorite has low permeability when encountered during drilling. Like the lopolith, flow in this igneous body must be fracture dominated and highly variable (Nordstrom et al., 1989).

Previous hydrochemical and $\delta D/\delta^{18}O$ investigations using several of the wells and springs reported in this paper were conducted by Bohm et al. (1980) and Karst et al. (1988). Our expanded data set has led to several conclusions that differ from these previous studies.

Chemical and Isotopic Characterization

Chemical Groups

Major ion chemical compositions are shown on a trilinear diagram in Figure 2. Waters from the SW and CAA ranges can be distinguished by high-Cl and high-HCO₃ fields respectively. Fluids from the DVGF lie in a low-(Ca, Mg) and high-Cl field. Hot spring and valley samples are not specifically associated with either field, although valley waters are more commonly associated with the CAA field. Only Dixie Hot Spring has major ion chemistry similar to thermal wells. The Cl-HCO₃-SO₄ triangular diagram is perhaps most diagnostic of water type (Fig. 2), and leads to a more general characterization of waters into High-HCO₃/Cl and Low-HCO₃/Cl groups (Fig. 3). A third trend of very high HCO₃/Cl also occurs.

The δD and $\delta^{18}O$ compositions of SW and CAA waters are similar, but are distinct from valley, hot spring, and reservoir fluids (Fig. 4). Isotopically heavy (less negative) δD and $\delta^{18}O$ compositions imply warmer conditions of recharge (summer, low altitude). Groundwater in the ranges would not be expected to be isotopically heavier than that in the valley. This occurrence suggests that the valley waters, including hot springs, were recharged during a colder climate. Noting similar relations in other Great Basin waters, Flynn and Buchanan (1993) suggest that the lighter waters are late-Pleistocene in age (10-30 ka). The position of pre-production reservoir fluid in Figure 4 is based on water collected in 1986-87. The position of the current reservoir average results from mixing with reinjection water that has become heavier due to evaporation in the cooling tower. The δD values of the reservoir fluids indicate that they are not fluids similar to those currently seen in the SW or CAA ranges. This does not mean that they were not recharged in the ranges, only that they were recharged during a colder climate. Likewise, the valley waters could have been recharged in the ranges during an earlier but cooler time.

Development of Chemical Compositions

Origin of Chloride. The sources of the Cl become apparent by examining $^{36}Cl/Cl$ (Fig. 5). Much of the Cl in the High-HCO₃/Cl waters was derived directly from precipitation (concentrated in soil by evaporation), as indicated by the nuclear weapons testing (high) $^{36}Cl/Cl$ ratios (Bentley et al., 1982). These waters, mostly CAA samples, must be younger than 50 years old. The Cl in the Low-HCO₃/Cl group, mostly SW and valley waters, was derived through a combination of pre-1950's precipitation ($^{36}Cl/Cl \approx 300E-15$; Bentley et al., 1986) and dissolution of Cl from rock (Fig. 5). Typical rock $^{36}Cl/Cl$ values are shown in Table 1. DVGF fluids have $^{36}Cl/Cl$ ratios of about $(51 \pm 3)E-15$ (based on analysis of 24 samples; see Fig. 5). The uniformity of the $^{36}Cl/Cl$ ratio suggests that this is the ratio in the rock from which their Cl was derived. The only lithology thought to abundantly occur in the subsurface with $^{36}Cl/Cl$ values typically of this magnitude is the Cretaceous granodiorite (Table 1; see Nimz et al., 1997)

Origin of Bicarbonate. Figure 6 shows $\delta^{13}C$, ^{14}C , and $^{87}Sr/^{86}Sr$ values that provide some information on HCO₃ origins for the Low-HCO₃/Cl and very high HCO₃/Cl groups. All very high HCO₃/Cl samples fall into the high $\delta^{13}C$ cluster on Figure 6. These samples appear to lie on a line between atmospheric values and values we have measured in Triassic marine limestones of the SW and CAA ranges. Low-HCO₃/Cl samples lie along another line between atmospheric $\delta^{13}C$ and a value intermediate between the limestones and fracture-fill vein calcite we have

measured from the SW range. All of the geothermal wells we have measured lie on the “calcite” line, while all of the hot springs except for Dixie Hot Springs lie on the “limestone” line. Most of the waters have interacted with subsurface carbonates that have added HCO_3 , altered the original atmospheric $\delta^{13}\text{C}$ values, and artificially increased their ^{14}C age. It is not completely apparent what the carbonate endmembers are, despite the measured limestone and calcite $\delta^{13}\text{C}$ values. First, the Br-Cl trend of the Dixie Valley samples is unlike the seawater trend (Fig. 3). Significant interaction with marine carbonates should produce a seawater Br-Cl trend. Second, the $^{87}\text{Sr}/^{86}\text{Sr}$ composition in the waters seems largely controlled by carbonate dissolution ($\delta^{13}\text{C}$; Fig. 6). Projecting the $^{87}\text{Sr}/^{86}\text{Sr}$ trend to an endpoint at the limestone $\delta^{13}\text{C}$ value produces a value of 0.7095. This is too high for Mesozoic or even Paleozoic seawaters (which are <0.7088), suggesting that the endmember may not be a marine carbonate (Burke et al., 1982).

Water Recharge Ages

More specific ages than those derived from $\delta\text{D}-\delta^{18}\text{O}$ can be estimated using ^{14}C , provided attention is paid to carbonate chemistry, especially $\delta^{13}\text{C}$ (Fig. 6). The oldest reliable measured CAA age is ~ 5 ka. However, the CAA $^{36}\text{Cl}/\text{Cl}$ values indicate *most* waters are <50 a. The oldest reliable SW range age is ~ 9 ka. Sample DV56, a SW cold spring, gives an uncorrected age of ~ 19 ka, and is sufficiently like valley hot springs in HCO_3 and $\delta^{13}\text{C}$ that it reasonably could be Pleistocene. Its δD value is low enough to make this plausible. The youngest reliable SW age based on ^{14}C is ~ 900 a, although a few bomb-pulse $^{36}\text{Cl}/\text{Cl}$ samples occur. It is noteworthy that very young waters are rare in the SW compared to the CAA range.

The oldest reliable age for a non-thermal water measured in the valley is ~ 14 ka (Shaw well; Fig. 6). Ages for samples reacting with subsurface carbonate can be regarded as *maximum* ages, since this process makes samples appear older. The maximum age for a valley hot spring is ~ 25 ka (Hyder), for a thermal well is ~ 31 ka (DF62-21), and for a DVGF production fluid is ~ 13 ka. A simple-minded reconstruction of their $\delta^{13}\text{C}$ values, following the limestone-calcite interaction lines on Figure 6, suggests these samples are 5-20 ka. However, this is probably over-simplified. The *youngest* maximum age for a hot spring sample is ~ 13 ka (Dixie), and for a thermal well is ~ 12 ka. Based on this evidence, the range in $\delta^{13}\text{C}$ values, and the $\delta\text{D}-\delta^{18}\text{O}$ values, it is reasonable to believe that most of the thermal water in the region is ~ 12 -14 ka. It is notable that the oldest reliable non-thermal valley age is of similar magnitude (Shaw well). It is perhaps also significant that two wells not in the DVGF have older max ages (DF62-21 and DF45-14).

Evidence of Water Mixing

Evidence of mixing between or within chemical/isotopic or age groups can be a guide to understanding hydrologic flow. Samples with intermediate chemical compositions are apparent on the figures. However, samples intermediate on one diagram are usually not those that are intermediate on other diagrams. Widespread mixing *between* groups is therefore not evident. *Within* groups, the system most suggestive of mixing is $^{36}\text{Cl}/\text{Cl}$. Figure 5 shows linear arrays radiating from a high-concentration/low-ratio composition, forming various trends. Mixing calculations indicate that the amounts of the high-Cl endmember are small. For example, the hot springs would be predominantly a low-Cl, presumably surface-water, endmember with small and variable amounts of a high-Cl, possibly reservoir-like, endmember: Lower Ranch $<3\%$, Jersey $<5\%$, Sou $\approx 5\%$, Hyder $\approx 5\%$, Dixie $\approx 25\%$. McCoy Hot Spring requires a significantly more concentrated surface-water endmember (~ 180 -210 mg/L Cl), although the mixing percentage would be similar to the other hot springs ($\sim 15\%$ reservoir-like water).

Chemical interaction with rock - Cl dissolution - would also produce similar arrays (Fig. 7). With the available data set, it is difficult to discriminate between mixing and dissolution processes for the Dixie Valley waters. The trajectories for samples within single chemical or age groups on Figure 7 are perhaps closer to the trajectories of the mixing lines, particularly at high Cl concentrations. For this reason it is felt that while rock interaction does occur, some mixing with high-Cl low- $^{36}\text{Cl}/\text{Cl}$ endmembers is partly responsible for producing the observed lower $^{36}\text{Cl}/\text{Cl}$ ratios *within* the SW, valley and hot springs groups.

Figure 7 also provides some insight into the origin and evolution of the low- $^{36}\text{Cl}/\text{Cl}$ endmember. Assuming the water recharged with an atmospheric $^{36}\text{Cl}/\text{Cl}$ ratio ($\sim 300\text{E}-15$), it must have begun reacting with rock when it still had a very low Cl concentration, similar to the valley Shaw well. That is, virtually none of the Cl was derived from the soil column where it was concentrated through evaporation (and still be $\sim 300\text{E}-15$). If it had originated with concentrations similar to SW range waters, where soil Cl must be a factor, the dissolution trajectories indicate it would not have achieved its present $^{36}\text{Cl}/\text{Cl}$ together with its present Cl concentration.

Observations and Implications

Based on the chemical and isotopic measurements, there are several observations that can be made concerning the relations among the hydrochemical groups and regional hydrologic flow.

Dixie Valley Regional Waters: Characterization and Chemical Relations

- Valley groundwaters, hot springs, and DVGF fluids recharged during colder conditions than SW-CAA waters, suggesting a late-Pleistocene age that is supported by ^{14}C ($\sim 12-14$ ka).
- Most of the water observed in the CAA range is very young, $<50\text{a}$.
- Most of the water observed in the SW range is much older than CAA water (e.g., ~ 9 ka), even though they have similar δD values.
- Some Pleistocene-age valley waters have remained or become very dilute (e.g., Shaw).
- The lowest- $^{36}\text{Cl}/\text{Cl}$ waters (DVGF fluids, DV56) may not derive the bulk of their Cl from their current host rocks, the Triassic marine sequences or Humboldt Lopolith. The only lithology in the region with $^{36}\text{Cl}/\text{Cl}$ similar to these waters is the Cretaceous granodiorite.
- $^{36}\text{Cl}/\text{Cl}$ modeling suggests that reservoir fluids evolved from dilute surface waters like those of the Shaw well, rather than from more concentrated surface waters like those in the SW range.
- $\delta^{13}\text{C}$ values suggest that the very high HCO_3/Cl group has interacted with marine carbonates; in comparison, based on $\delta^{13}\text{C}$ -calcite trends, the low- HCO_3/Cl group apparently has not.
- Very limited mixing *between* chemical groups may occur. *Within* groups, internal mixing with low- $^{36}\text{Cl}/\text{Cl}$ endmembers (DVGF- or DV56-like fluids) appears more common.

Regional Fluid Flow: Origins, Relative Rates, and Flowpaths

- If the Cl in the reservoir fluids is derived from granodiorite, then either this rock occurs at depth beneath the valley, the bulk of the Cl is incorporated within the fault zone at the granodiorite contact, or fluid flow is across the SW fault zone.
- Average subsurface flow from the ranges into the valley is not rapid; valley water is still Pleistocene in age. Simplistic flow-line analysis would suggest $<1\text{m/a}$ flow rates.
- Controls on flow paths vary greatly within the regional hydrologic system. Evidence includes:
 - Artesian dilute Shaw-type waters and the DVGF fluids are the same age.
 - Flow rates to reservoir depths exceed 0.25m/a , assuming 3000m depth and an age of 12 ka.
 - Flow rates to valley shallow domestic wells are $<0.03\text{m/a}$, assuming vertical piston flow, $<300\text{m}$ depth, and an age of 12 ka (non-vertical flow paths require even slower flow rates).

- Old ages and high-TDS in SW waters suggest a deep source and a regional upward hydrologic gradient with an axis in the SW range; this may also affect the valley.
- Despite the upward gradient, hot springs contain only a small fraction of reservoir-like water.

Acknowledgments

This research was supported by the Geothermal Technology Division under the Assistant Secretary for Energy Efficiency and Renewable Energy of the U.S. Department of Energy. We thank Oxbow Power Services Incorporated, and Dick Benoit in particular, for very significant help with field work logistics, background chemical data, and providing access to geothermal field wells. Work by LLNL authors was performed under the auspices of the U.S. Department of Energy by Lawrence Livermore National Laboratory under contract W-7405-Eng-48.

References

- Bell, J.W. and Katzer, T. (1990) Timing of late Quaternary faulting in the 1954 Dixie Valley earthquake area, central Nevada. *Geology*, 18:622-615.
- Bentley, H.W., Phillips, F.M., and Davis, S.N. (1986) Chlorine-36 in the terrestrial environment. In: P. Fritz and J.-Ch. Fontes (Editors), *Handbook of Environmental Geochemistry*. Elsevier, Amsterdam. p. 427-480.
- Bentley, H.W., Phillips, F.M., Davis, S.N., Gifford, S., Elmore, D., Tubbs, L.E., and Gove, H.E. (1982) Thermonuclear ^{36}Cl pulse in natural waters. *Nature*, 300: 737-740.
- Bohm, B.W., Jacobson, R.L., Campana, M.E., and Ingraham, N.L. (1980) Hydrology and Hydrogeochemistry. In: *Geothermal Reservoir Assessment Case Study, Northern Basin and Range Province, Northern Dixie Valley, Nevada*. Mackey Minerals Research Institute, v.1, p. 159-186.
- Burke, W.H., Denison, R.E., Hetherington, E.A., Koepnick, R.B., Nelson, H., and Otto, J.B. (1982) Variation of seawater $^{87}\text{Sr}/^{86}\text{Sr}$ throughout Phanerozoic time. *Geology*, 10:516-519
- Flynn, T. and Buchanan, P.K. (1993) Pleistocene origin of geothermal fluids in the Great Basin, western United States. *Resource Geol. Spec. Issue*, 16:60-68.
- Karst, G.B., Campana, M.E., and Jacobson, R.L. (1988) A mixing-cell model of the hydrothermal flow system, northern Dixie Valley, Nevada. *Geothermal Resources Council Transactions*, 12:167-174.
- Kennedy, B.M., Janik, C., Benoit, D., and Shuster, D.L. (1999) Natural geochemical tracers for injectate fluids at Dixie Valley. *Proceeding of the 24th Workshop on Geothermal Reservoir Engineering, Stanford University*.
- Nimz, G.J., Moore, J.N., and Kasameyer, P.W. (1997) $^{36}\text{Cl}/\text{Cl}$ ratios in geothermal systems: Preliminary measurements from the Coso field. *Geothermal Resources Council Transactions*, 21:211-217.
- Nordstrom, D.K., Olsson, T., Carlsson, L., Fritz, P. (1989) Introduction to the hydrogeological investigations within the International Stripa Project. *Geochim. et Cosmochim. Acta* 53:1717-1726.
- Okaya, D.A. and Thompson, G.A. (1985) Geometry of the Cenozoic extensional faulting, Dixie Valley, Nevada. *Tectonics* 4:107-125.
- Parchman, W.L. and Knox, J.W. (1981) Exploration for geothermal resources in Dixie Valley, Nevada. *Geothermal Resources Council Bull.* June, 1991.
- Speed, R.C. (1976) *Geologic Map of the Humboldt Lopolith*, scale 1:81050, GSA Map Chart Series, MC-14.
- Thompson, G.A. and Burke, D.B. (1973) Rate and direction of spreading in Dixie Valley, Basin and Range Province, Nevada. *Geol. Soc. Am. Bull.* 84:627-632.
- Williams, C.F., Sass, J.H., and Grubb, F.V. (1997) Thermal signature of subsurface fluid flow in the Dixie Valley geothermal field, Nevada. *Stanford Geothermal Workshop Proceedings, SGP-TR-155*, 22:77-85.

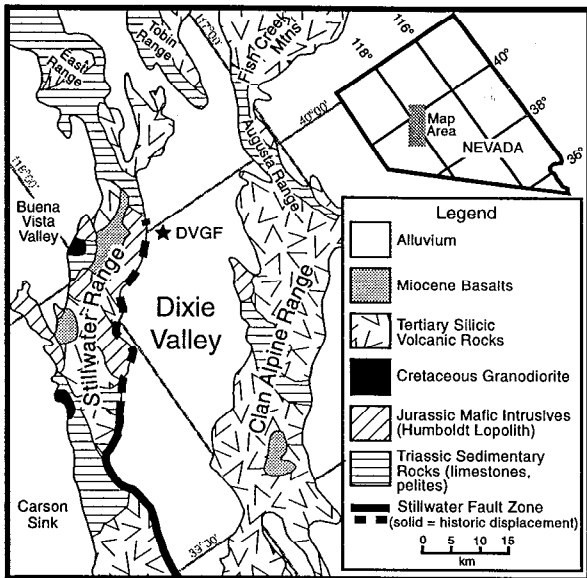


Figure 1. Dixie Valley Region. Water samples collected throughout map area. DVGF = Dixie Valley Geothermal Field.

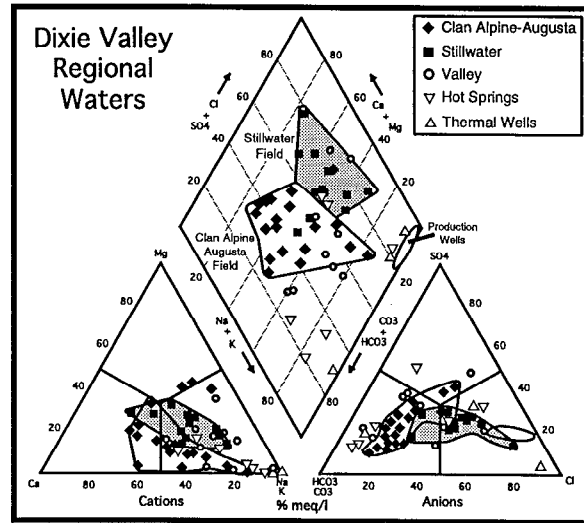


Figure 2. Trilinear diagram showing major ion relationships of the Dixie Valley regional waters. Thermal wells shown are wells not in production at the DVGF.

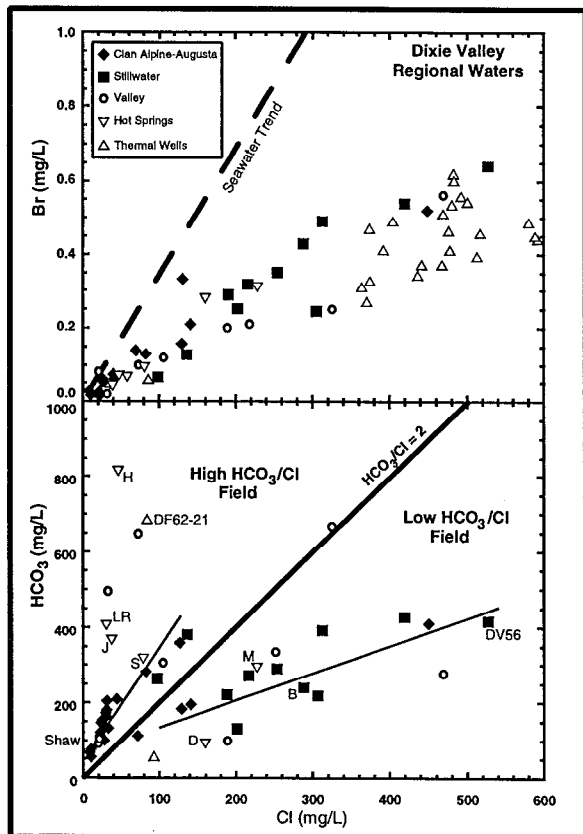


Figure 3. Bicarbonate-chloride-bromide relations for Dixie Valley regional waters. DVGF production wells not plotted on $\text{HCO}_3\text{-Cl}$ diagram. Select wells and springs discussed in text are identified. B = Bolivia artesian well. Hot springs: D = Dixie, H = Hyder, J = Jersey, LR = Lower Ranch, M = McCoy, S = Sou.

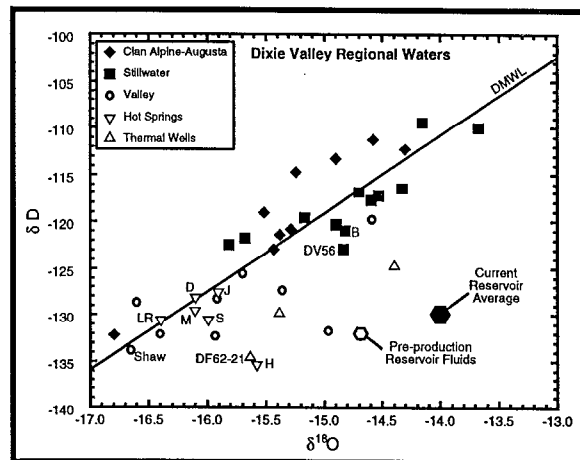


Figure 4. Oxygen-hydrogen isotopic compositions of Dixie Valley regional waters. The Dixie Valley meteoric water line (DMWL) represents the linear regression through SW, CAA, and valley waters. Sample identifiers are the same as Figure 3.

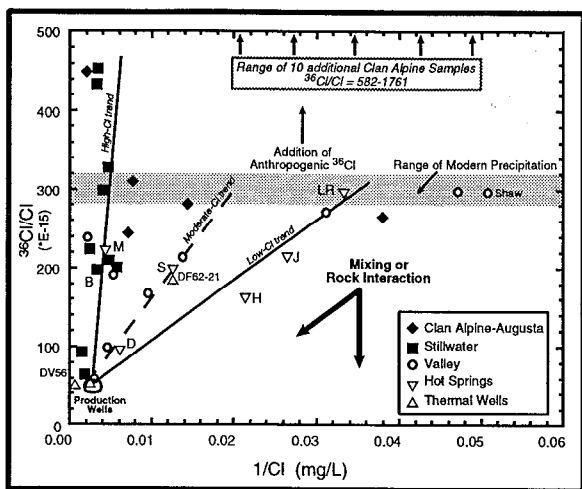


Figure 5. Chloride- $^{36}\text{Cl}/\text{Cl}$ relationships in Dixie Valley regional waters. Range for modern precipitation represents expected variation of $^{36}\text{Cl}/\text{Cl}$ ratios in precipitation chloride based on calculations of Bentley et al. (1986), and direct measurement of one Dixie Valley rain sample. The range is not intended to represent the range of precipitation Cl concentration. Anthropogenic ^{36}Cl represents globally distributed ^{36}Cl due to nuclear weapons testing, 1950's-60's. Sample identifiers are the same as Figure 3.

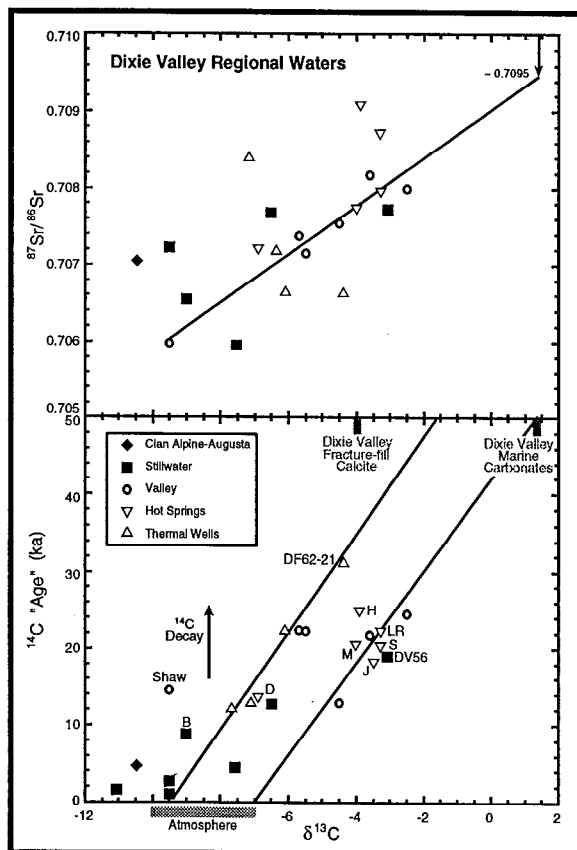


Figure 6. $\delta^{13}\text{C}$ - ^{14}C - Sr isotope relations in Dixie Valley regional waters. ^{14}C "age" positioning of carbonate and calcite endmembers represents the approximate upper age limit of detection for the ^{14}C technique (~50 ka). Samples with $\delta^{13}\text{C}$ values more negative than atmosphere indicate addition of biologically mediated carbon. Sample identifiers are the same as Figure 3.

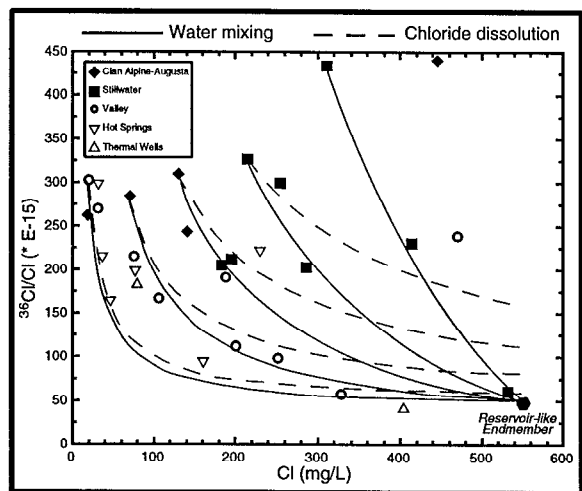


Figure 7. Mixing and Cl dissolution curves for various Dixie Valley water endmembers. Low- $^{36}\text{Cl}/\text{Cl}$ endmember represents reservoir-like fluid compositions, but with chloride contents higher than pre-production values (see Kennedy et al., 1999). Cl dissolution curves are not a function of the Cl concentrations in the "rock" endmember, since the model adds chlorine until reservoir $^{36}\text{Cl}/\text{Cl}$ values are achieved (curves continue off of diagram to higher Cl contents). Measured Dixie Valley samples are used for high- $^{36}\text{Cl}/\text{Cl}$ endmembers.

Table 1
Characteristic $^{36}\text{Cl}/\text{Cl}$ values of common rocks

| Rock: | | Basalt | Andesite | Granitic | Rhyolite | Arkose | Limestone | Shale |
|-----------------------------------|--------------------------------|--------|----------|----------|----------|--------|-----------|-------|
| neutron producers | SiO %ox | 49.5 | 59.0 | 67.2 | 67.2 | 77.1 | 0.8 | 62.8 |
| | Al ₂ O ₃ | 15.0 | 17.4 | 16.0 | 16.0 | 8.7 | 0.3 | 18.9 |
| | MgO | 6.5 | 3.5 | 1.8 | 1.8 | 0.5 | 2.1 | 2.2 |
| | Na ₂ O | 3.0 | 3.5 | 3.8 | 3.0 | 1.5 | 0.0 | 1.2 |
| | K ₂ O | 1.0 | 1.4 | 2.8 | 2.2 | 2.8 | 0.0 | 3.7 |
| | F ppm | 200 | 350 | 700 | 600 | 220 | 112 | 560 |
| | Th | 3.0 | 6.9 | 18.7 | 16.8 | 5.7 | 2.0 | 14.6 |
| U | 0.8 | 1.8 | 5.8 | 5.3 | 1.5 | 1.0 | 3.1 | |
| neutron absorbers | Li | 16 | 20 | 40 | 32 | 15 | 5 | 75 |
| | B | 5 | 15 | 15 | 12 | 35 | 55 | 100 |
| | Sm | 5.0 | 3.5 | 4.2 | 3.4 | 3.1 | 3.8 | 5.6 |
| | Gd | 5.0 | 3.3 | 4.2 | 3.4 | 2.7 | 3.8 | 4.7 |
| neutrons/cm ² / a | | 449 | 1184 | 3293 | 3142 | 715 | 274 | 1095 |
| $^{36}\text{Cl}/\text{Cl}$ (E-15) | | 6.5 | 17.1 | 47.5 | 45.3 | 10.3 | 4.0 | 15.8 |